Structural and Thermal Analysis of Heat Exchanger with Tubes of Elliptical Shape

By

Nawras H. Mostafa **Qusay R. Al-Hagag**

Abstract:

An approach to select the tube wall thickness distribution of streamlined tubes intended for use in heat exchangers is developed in this study. The main goal is to retain a streamlined outer profile (resist deformation) and to prevent strain failure due to the applied internal pressure. The effect of the tube wall thickness distribution on shaped tube efficiency is also considered. The strain is calculated as a function of several dimensionless geometric ratios and the ratio of the internal pressure to elastic material modulus. Using the finite element method, a set of dimensionless design curves is created for elliptical tube geometries. From these curves, a range of possible materials and tube geometries can be selected that meet a specific strain limit. To illustrate the approach, structure-satisfied elliptical designs are selected and their thermal performance is evaluated for an automotive charge air cooler made of polymeric material.

التحليل التركيبي و الحراري لمبادل حراري ذو أنابيب بيضوية الشكل

نورس حيدر **قصي رشيد**

الخلاصة

تتضمن هذه الدراسة تسهيل عملية اختيار توزيع سمك جدار الأنبوب لمنظومة الأنابيب الانسيابية المستخدمة في المبادلات الحرارية. إن الهدف الرئيسي هو الحفاظ على الشكل الانسيابي الخارجي للأنابيب (أي مقاومة التشوه) ومنع الانهيار الانفعالي نتيجة للضغط المسلط داخل تلك الأنابيب.كما تم دراسة تأثير توزيع سمك جدار الأنبوب على كفاءته (الكفاءة الحرارية).تم حساب الانفعال كدالة لنسب هندسية لا بعديه بالاضافة إلى نسبة الضغط الداخلي إلى معامل المرونة لمادة الأنبوب. تم استخدام طريقة العناصر المحددة لإيجاد مجموعة من منحنيات التصميم اللابعدية الخاصة بالأنابيب البيضوية المقطع. هذه المنحنيات، أعطت مدى لأختيار المادة و الشكل الهندسي المحدد بانفعال معين. و لتوضيح هذه الطريقة تم اختيار مبردة هواء الشحن في السيارة ذات أنابيب بيضوية الشكل مصنعة من مادة لدائنية لتحقيق التصميم البنيوي و تخمين الأداء الحراري لها.

Keywords: elliptical tube, shaped tube efficiency, polymer, heat exchanger, deformation, strain, stress

1- Introduction

Polymer heat exchangers have been used for decades in corrosive environments [1–4] and are now being considered in other applications where either weight is a concern or innovative geometries are desirable. The most common polymer heat exchanger is a tube bundle made of hundreds of circular tubes connected to headers. Elliptical and lenticular profiles are being considered due to their ability to reduce form drag over a wide range of flow rates [6–12]. There are three primary challenges to design the streamlined tubes:

a. The tube wall thickness distribution (i.e. the geometry of the inner flow passage) must be selected so that the maximum stress in the tubes is less than the mechanical strength of the material.

b. The deformation of the tubes must be within a range to avoid strain failure and to maintain a streamlined profile.

c. The tube wall thickness distribution should be selected to reduce the wall thermal conductive resistance.

For polymers, which have low thermal conductivity and strength compared with metals, there is a significant trade-off between the thermal performance and the mechanical design requirements. Based on earlier work [13], it is anticipated that a non-uniform wall distribution will emerge as the optimum solution.

Two mechanical failure modes must be considered: burst failure and strain failure [14]. Because polymers creep, a strain limit may be exceeded before the stresses exceed the burst strength. Young's modulus for polymeric material is significantly lower than those for most metals. Consequently, for the same loading, a polymer structure must be thicker than a metal structure to avoid strain failure.

Stress distribution and deformation in circular and elliptical tubes with uniform wall thickness are well understood. Exact solutions of stress distribution and deformation in internally pressurized circular tubes are available in standard reference texts (see, for example, reference [15]). The hoop and radial stresses are axisymmetric; there is only radial displacement. Stresses and deformation have also been analyzed for non-circular tubes, primarily elliptical tubes [16–18]. In elliptical tubes, stresses concentrate at the major and minor axes [16] and deformation is non-uniform [17, 18].

The use of a non-uniform wall to reduce stress in elliptical tubes was proposed by Holland [13]. He identified optimum wall thickness distributions to minimize the maximum bending stress for minor to- major-axis ratios from 0.1 to 1.0. The geometry that he proposed has the maximum thickness at the major axis and the minimum thickness at the minor axis. His analysis is based on a beam approximation which is limited to thin-walled tubes with small deformations.

The objective of the present study is to develop an approach to optimize the inner flow passage of streamlined polymer tubes intended for use in heat exchangers. The goal is to retain a streamlined outer profile (resist deformation) and to prevent failure due to the pressure imposed by the heat transfer fluid flowing in the tube. Dimensionless parameters are utilized throughout the analysis such that the results are applicable to elliptical tubes of all sizes. This approach can be extended to other outer shapes.

2- Approach

The effect of the inner geometry and tube wall thickness on stress and deformation of elliptical tubes was determined numerically using finite element analysis for internally pressurized tubes. Several dimensionless geometric parameters are required to define the relative size and shapes of the outer and inner ellipses (Fig. 1):

(a) λ_o, the length ratio of the minor axis to major axis of the outer ellipse.

(b) λ_i, the length ratio of the minor axis to major axis of the inner ellipse.

(c) λ_t, the length ratio of the wall thickness at $\theta = 90^o$ to the semi minor axis of the outer ellipse.

The optimum inner shape is one in which the stresses and strains are within material limits and the heat transfer is greatest. To select an optimum inner shape for a fixed outer shape λ_o , a two-step approach is undertaken. The stress and strain limits are imposed and a set of acceptable inner ellipses (λ_i and corresponding λ_t) are identified. From this set, the inner shape that maximizes the thermal performance for a specific application may be selected.

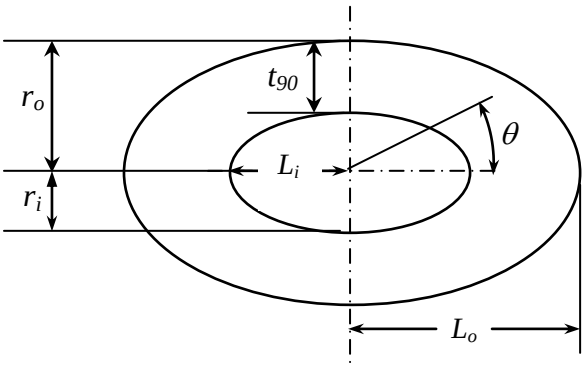

Fig. 1 Shaped elliptical tube.

For polymer tubes, the stress failure criterion is the hydrostatic burst strength [19] measured under temperature and pressure conditions similar to those of the application. The strain failure criterion was selected to limit the deformation of the tube. A strain limit of 0.05 is specified in the hydrostatic burst test, such that the burst strength is defined by either the pressure at which the tube ruptures or the pressure at which the tube strain reaches 0.05. Because polymers creep, the 0.05 strain limit is often exceeded before the tube ruptures. Thus, a maximum von Mises strain $\varepsilon_{\max}$ of 0.05 was selected as the criterion for selecting inner elliptical shapes which satisfy the mechanical failure requirements. It will be shown that by limiting the von Mises strain to less than $\varepsilon_{\max}$, the tube will remain streamlined even after deformation.

The strain within the tube was determined by solving the force equilibrium equations for a tube subjected to internal pressure P_i. Because the tube geometry is complex, the solution to the equilibrium equations was obtained by the finite element method. Regardless of the solution approach, the tube geometry, material properties, loads, and boundary conditions must be specified. The strain is reported in the form of $\varepsilon_{\max} E/P_i$ as a function of dimensionless parameters λ_i, λ_o, and λ_t. The range of values for each parameter was selected to ensure that the results are applicable to a wide range of materials, geometries, and loading conditions.

2.1- Tube geometry and boundary conditions

Two-dimensional elliptical tubes were drawn using ANSYS. Taking advantage of the tube symmetry, one-quarter of the tube shape was drawn in the x–y plane (**Fig. 2**) and meshed with the four-node element for plane stress **PLANE42**. This plane stress element has two degrees of freedom, the displacement in the x and y directions, at each node. A typical quarter-model of the elliptical shape required approximately 2000 elements. Mesh density was varied to determine the appropriate number of elements for convergence.

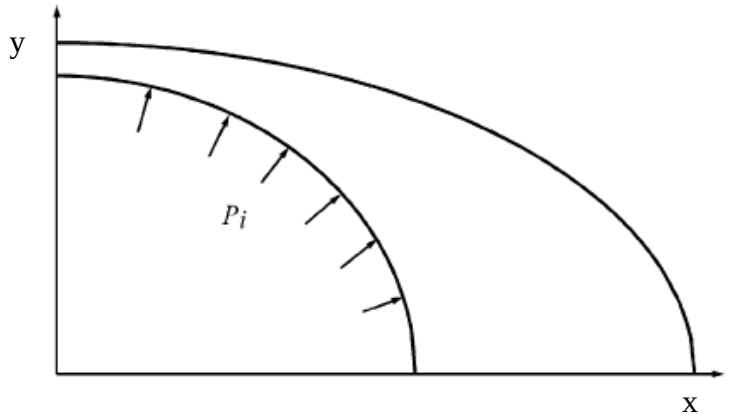

Fig.2 Quarter-model of an elliptical tube.

Tubes of varying geometries were modeled by changing the dimensionless length ratios λ_o, λ_i, and λ_t (Table 1). Specifically, three outer geometries are considered: λ_o = 0.3, 0.5, and 0.8 with four inner elliptical shapes are considered: λ_i = 0.3, 0.5, 0.8, and 1.0. The relative size of the inner to outer ellipse is determined by λ_t, which was varied from 0.04 to 1.0. As these parameters are decreased, the ellipse becomes more slender. A uniformly distributed constant pressure P_i was applied normal to the inner elliptical surface. At the outer elliptical surface, the pressure was set to zero.

2.2-Material properties

The material is modeled to be linear elastic. Only Young's modulus E and Poisson's ratio v are required to define the material stress–strain relationship. This material model is valid for most metals and for polymers loaded within the linear viscoelastic range. In this study, a polymer tube material is considered. Nylon (PA) material is considered for polymer heat exchangers. Long-term viscoelastic properties for these materials have been recently published [14]. The module of this polymer is 182 MPa for PA in air which represents the high value found among plastics. Aluminum and copper, with module of 7.3 * 10^4 MPa and 1.3 *10^5 MPa respectively, are metals often used in heat exchangers. To account for the performance of both metals and polymers over a range of operating conditions, the dimensionless parameter E/P_i was varied from 20 to 1000. Poisson's ratio for the material was set to 0.45 (that of polymers) regardless of the value of E/P_i.

Table 1 Inputs to the finite element model

Parameter	Value
Outer elliptical shape λ_o	0.3, 0.5,0.8
Inner elliptical shape λ_i	0.3, 0.5, 0.8, 1
Relative size λ_t	0.04-1
Modulus/load E/P_i	20-1000
Poisson's ratio v	0.45

2.3- Finite element output

Since a strain failure criterion is imposed, the maximum von Mises strain ε_{max} is calculated as part of the post-processing option in ANSYS. Because a linear material constitutive law was adopted, the strain results can be represented by the dimensionless parameter $\varepsilon_{max} E/P_i$. This parameter is a variation of the dimensionless parameter σ_{max}/P_i, which is often used for linear elastic materials in which the stresses σ vary linearly with the load. Displacement is also of interest, particularly in the case of polymer tubes. Large displacement of the tube indicates that the tube may take a new shape and subsequently heat transfer and pressure drop will be affected.

2.4-Shaped tube efficiency

The shaped tube efficiency is defined as

$$\eta \equiv \frac{q}{q_{max}} = \frac{\overline{T_o} - T_\infty}{\overline{T_i} - T_\infty} \qquad (1)$$

where q is the actual heat transfer rate of the shaped tube and q_{max} is the heat transfer rate that would be achieved if the spatially averaged temperature of the surface of the shaped tube, $\overline{T_o}$, were equal to the average temperature of the base of the fin, $\overline{T_i}$ at $r = r_i$ [5].

3- Results and discussion

The effect of tube geometry, materials, and loading on tube strain is illustrated in Fig. 3. This set of graphs shows the thickness ratio λ_t as a function of $\varepsilon_{max} E/P_i$. The three plots correspond to three different values of λ_o (0.3, 0.5, and 0.8). Model output for each inner elliptical shape (λ_i = 0.3, 0.5, 0.8, and 1.0) are shown as solid curves on each plot. For $\varepsilon_{max} E/P_i$ < 15, the thickness ratio decreases significantly with increasing . For $\varepsilon_{max} E/P_i$ > 40 the thickness ratio remains fairly constant and approaches a minimum for each inner shape.

Given an application and material, tube shapes which satisfy a particular strain failure criterion can be identified as follows. The value of $\varepsilon_{max} E/P_i$ is defined by the pressure requirements of the application, the material modulus, and the strain failure limit. A vertical line passing through this ratio intersects each λ_i curve for a selected value of λ_o. For the selected λ_i, a corresponding value of λ_t is shown on the ordinate. Thus, the sets of dimensionless geometry parameters λ_o, λ_i, and λ_t, which satisfy the strain limit for a particular application, can be identified.

To illustrate the use of plots, consider an application in which the strain limit is 0.05 and $E=P_i$ is 600 ($\varepsilon_{max} E/P_i$ = 30). Then, the results shown in **Fig. 3** can be plotted on a single graph (**Fig. 4**). The curves correspond to outer elliptical shapes of λ_o = 0.3, 0.5, and 0.8. Regardless of the outer shape, λ_t decreases with increasing λ_i. Each curve represents combinations of thickness and inner shape that meet the pressure and strain limit requirements. For a particular outer shape (λ_o), there are many combinations of thickness and inner shape from which to choose. As expected, the circular tube requires the thinnest wall. However, the circular tube produces the greatest form drag and may not provide the maximum heat transfer.

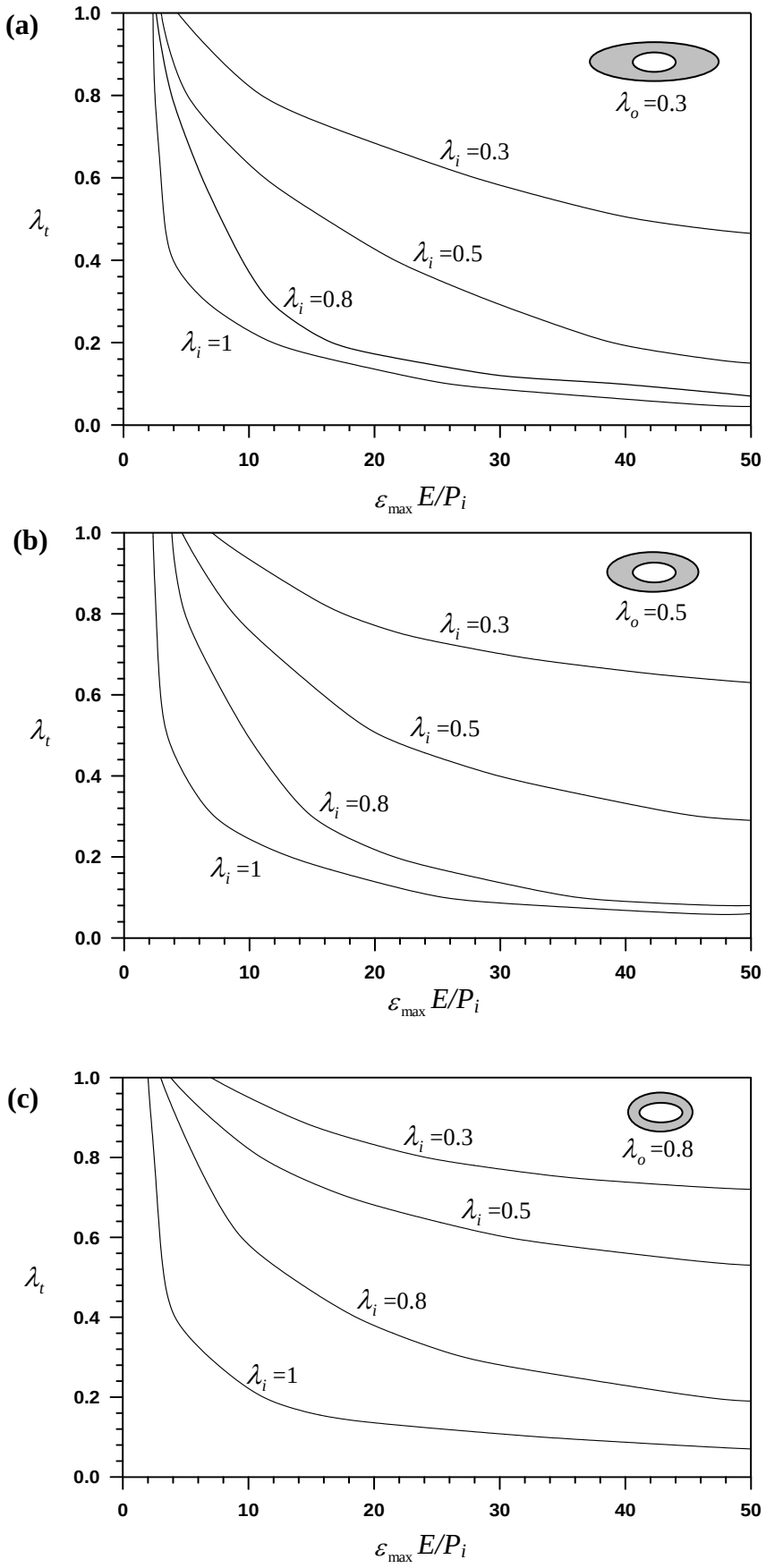

Fig. 3 Selection of the thickness ratio λ_t for the specified values of $\varepsilon_{\max} E/P_i$ for elliptical tubes with λ_i = 0.3, 0.5, 0.8, and 1.0 at **(a)** λ_o = 0.3, **(b)** λ_o = 0.5, and **(c)** λ_o =0.8

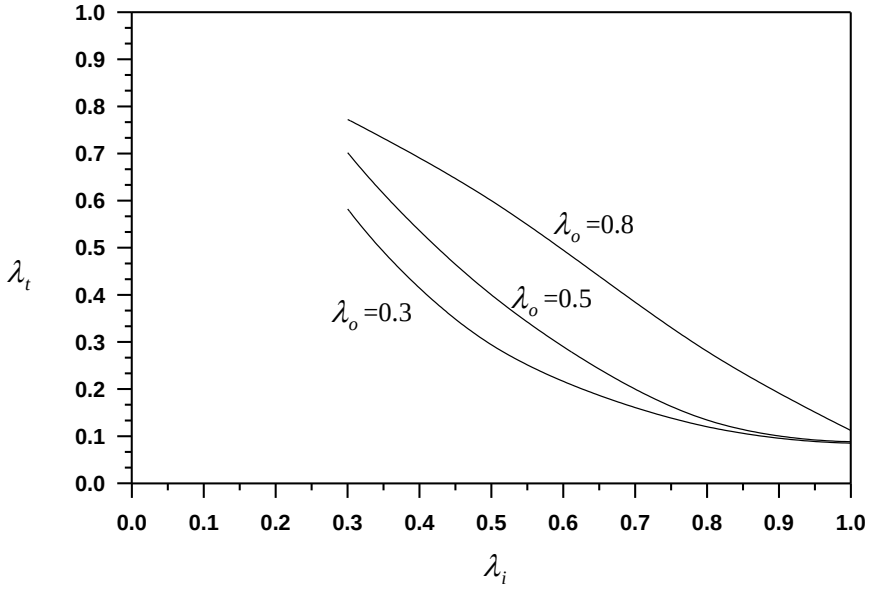

Fig. 4 Specification of λ_t corresponding to a selected λ_i for tubes with λ_o =0.3, 0.5, and 0.8 based on a maximum strain of 0.05 and E/P_i =600 (v=0.45)

The effect of tube shape on deformation is illustrated in **Fig. 5** for E/P_i = 600. **Fig. 5(a)** to **(e)** are tube designs based on a strain limit of 0.05 and **Figs 5(f)** and **(g)** are tube designs based on a strain limit of 0.10. The outer elliptical shapes shown are for λ_o =0.5 and 0.8, and the inner shapes are for λ_i =0.5 and 1.0.

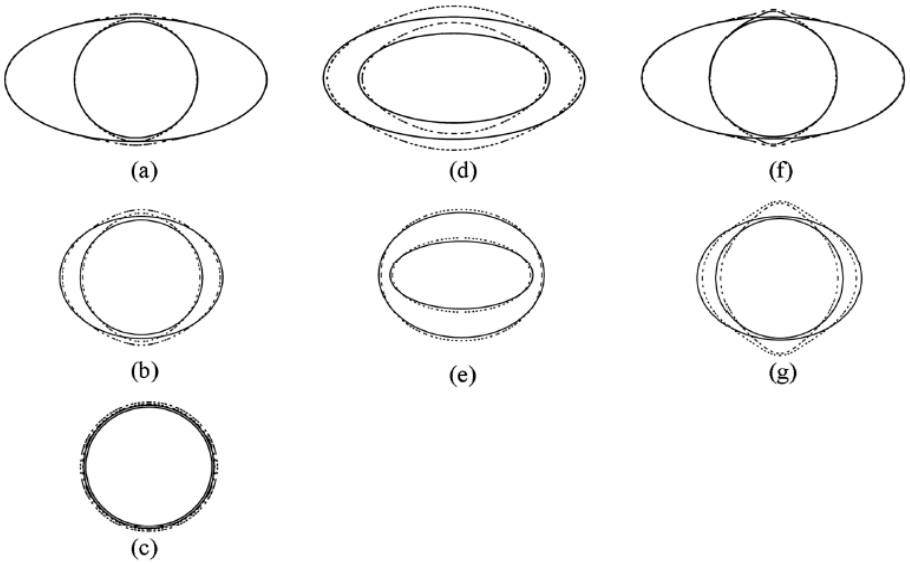

Fig. 5 Tube deformation for 0.05 strain with E/P_i = 600 (v=0.45): —, original tube geometry; - - -, deformed tube geometry. The figures shown in (a) to (e) are tube designs selected on the basis of 0.05 strain: (a) λ_o = 0.5 and λ_i =1; (b) λ_o =0.8 and λ_i =1; (c) circular tube with λ_o = λ_i =1; (d) λ_o = 0.5 and λ_i =0.8; (e) λ_o =0.8 and λ_i =0.8. The figures shown in (f) and (g) are tube designs based on 0.10 strain: (f) λ_o =0.5 and λ_i =1; (g) λ_o = 0.8 and λ_i =1.

The outer elliptical shapes shown are for λ_o =0.5 and 0.8, and the inner shapes are for λ_i =0.5 and 1.0. In contrast with a circular tube [**Fig. 5(c)**], when the outer shape is an ellipse, the deformation is not uniform and is greatest at the minor axis, $\theta = \pm 90^o$. The effect of the strain limit

on the outer profile is illustrated by comparing the deformation of an elliptical tube at 0.05 strain with that at 0.10 strain. Comparing **Fig. 5(a)** with **Fig. 5(f)**, which both have λ_o =0.5 and λ_i =1.0, it is shown that, when the strain limit is 0.05, the streamlined shape is maintained. When the strain limit is 0.10, the deformation at the minor axis is significant, creating a sharp protrusion at $\theta = \pm 90^o$ that is expected to increase form drag.

4- Case study

The final selection of tube geometry depends on the required thermal duty of the tubes and the operating conditions. Case studies are presented for an automotive charge air cooler and radiator made of nylon tubes. In this exercise, the tube is assumed to have λ_o =0.5 with a fixed outer radius r_o = 2mm, representative of nylon circular tubes made by a major polymer manufacturer. The inner shape is selected with the criteria of 0.05 strain and maximum heat transfer rate. Two tubes are considered. Tube A has a circular inner flow passage (λ_i =1), and tube B has an elliptical inner flow passage with λ_i =0.5.

Nominal operating conditions for the two heat exchangers are provided in **Table 2**. For these conditions, $\varepsilon_{\max} E/P_i$ for 0.05 maximum strain is 30 for the charge air cooler. The module of nylon are assumed to be 182 MPa in air. **Table 3** provides the required λ_t, determined from **Fig. 3(b)**, together with the specified geometric parameters.

Table 2 Nominal operating conditions of an automotive charge air cooler [6]

Automotive application	Surface	Fluid	T_{outer} (^{o}K)	T_{inner} (^{o}K)	U (m/s)	P_i (MPa)
Charge air cooler	Outer	Air	298	400	8	0.3

Table 3 Charge air cooler and radiator tube geometry based on a strain limit of 0.05. Tube A has a circular inner flow passage (λ_i =1) and tube B has an elliptical inner flow passage (λ_i =0.5)

		Specified geometric parameters				Calculated dimensions			
Application	Tube	r_o (mm)	λ_o	λ_i	λ_t	L_o (mm)	r_i (mm)	L_i (mm)	A_i (mm^2)
Charge air cooler	A	2	0.5	1	0.084	4	1.83	1.83	10.52
Charge air cooler	B	2	0.5	0.5	0.4	4	1.2	2.4	9.04

The heat transfer rate is determined numerically using the commercial software ANSYS. The temperature distribution is computed by solving the two-dimensional conduction problem across the elliptical tube wall. The heat transfer rate per unit length tube is calculated by integrating the heat flux over the surface of the tube according to

$$Q = \int_{\theta=0}^{2\pi} q.r.d\theta \qquad (2a)$$

where q is the heat flux calculated from the temperature gradient on the tube wall surface

$$q = -k_w \left(\frac{\partial T}{\partial n} \right)_{wall} \qquad (2b)$$

and k_w is the thermal conductivity of the material. The thermal conductivity of the nylon is assumed to be 0.24W/mK. Fluid properties are evaluated at the inlet temperature and pressure. Triangular meshes were refined until the heat transfer rate varied less than 0.01. Heat transfer coefficients, will calculate from equations (3a), (3b), and (4), are applied as boundary conditions at the outer and inner surface of the tubes.

The heat transfer coefficients are assumed to be uniform along the outer and inner heat transfer surfaces. The outer overall convective heat transfer coefficient h_o is determined from a Nusselt number correlation for a circular and an elliptical tube [12] according to

$$Nu_{2L_o} = 0.27\,\mathrm{Re}_{2L_o}^{0.6}\,\mathrm{Pr}^{0.37}\left(\frac{\mathrm{Pr}}{\mathrm{Pr}_w}\right)^{0.25}$$

$$2000 \le \mathrm{Re}_{2L_o} \le 2*10^4 \qquad (3a)$$

and

$$h_o = \frac{Nu_{2L_o} k_f}{2L_o} \qquad (3b)$$

The overall convective heat transfer coefficient in the tubes is determined assuming a uniform heat flux boundary. For these tubes and operating conditions, flow in the tube is laminar. For fully developed laminar flow in an elliptical channel [20],

$$Nu_{D_h} = \frac{6}{11}\left[\frac{D_h}{r_i}\right]^2 (1+\lambda_i^2) \qquad (4a)$$

In this expression, the hydraulic diameter D_h equal to

$$D_h = \frac{4A_i}{P_{inner}} = \frac{2r_i L_i}{\sqrt{0.5(r_i^2 + L_i^2)}} \qquad (4b)$$

Heat transfer rates expressed per unit length of tube are presented in **Fig. 6**. For the charge air cooler, the tube with an elliptical inner flow passage provides slightly improved performance compared with the tube with the circular flow passage.

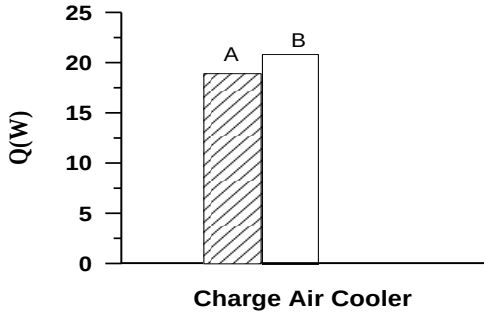

Fig.6 Heat transfer rate of an elliptical tube with λ_o=0.5 with a circular inner channel (A) and an elliptical inner channel (B) with λ_i=0.5 in an automotive charge air cooler (E/P_i=600).

In general, it may be concluded that, if conduction across the polymer wall poses the dominant thermal resistance, optimum thermal performance for a specified strain limit and outer shape is obtained by selecting the tube geometry which minimizes the amount of polymeric material; i.e. the shape of the inner flow passage with the greatest cross sectional area should be selected. On the other hand, if the dominant thermal resistance is the convective heat transfer inside the tube,

optimum performance is achieved by selecting the inner shape that provides the maximum heat transfer surface area; i.e. the shape with the greatest perimeter should be selected. To help guide the selection of inner tube geometry for thermal design, **Fig 7** show plots of shaped tube efficiency for shaped elliptical tubes with λ_o = 0.3, 0.5, and 0.8 .

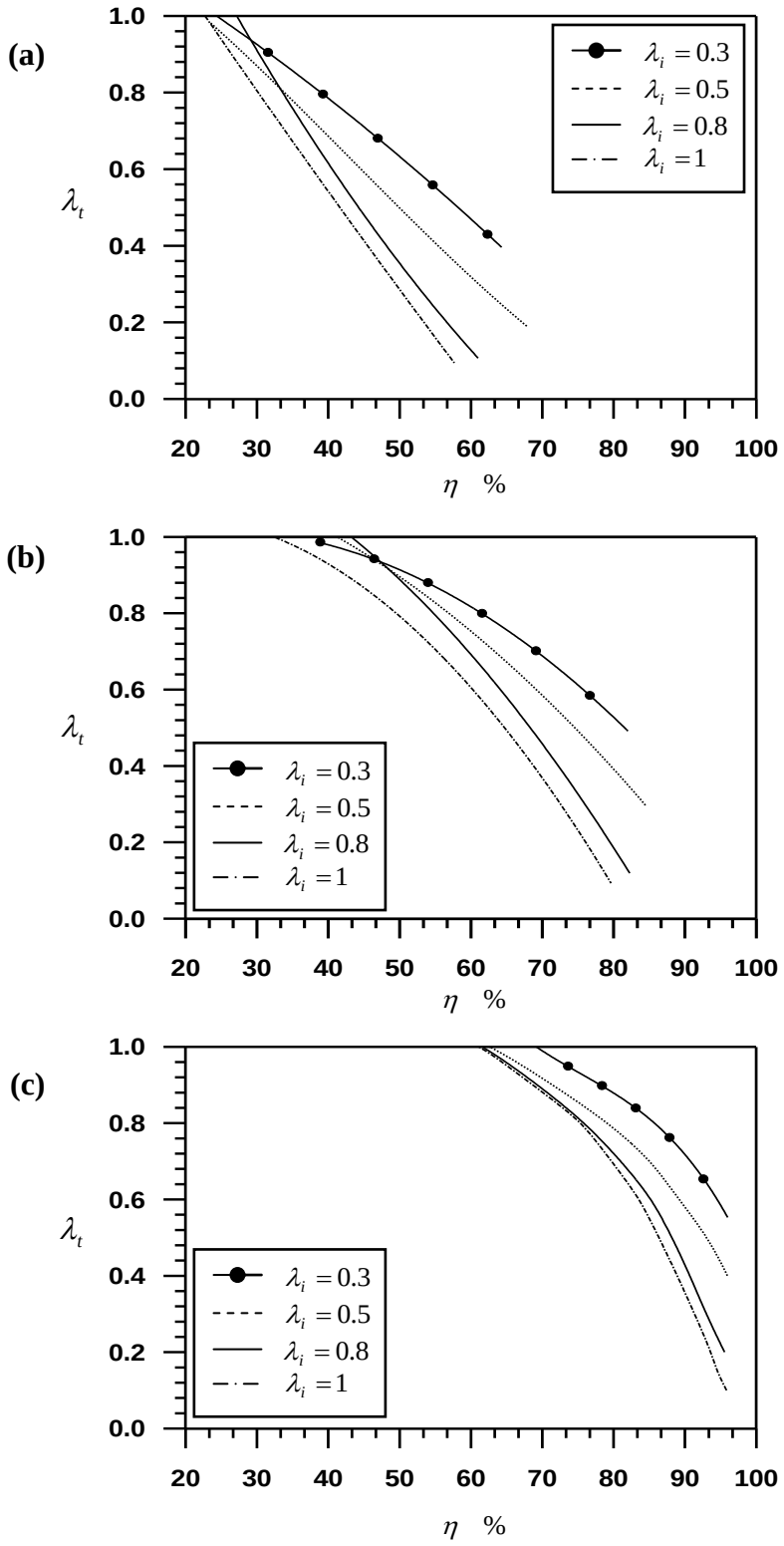

Fig. 7 thickness ratio λ_t with shape tube efficiency η for elliptical tubes with λ_i = 0.3, 0.5, 0.8, and 1.0 at **(a)** λ_o = 0.3, **(b)** λ_o = 0.5, and **(c)** λ_o =0.8

5- Conclusions

A method for analyzing the mechanical and thermal performance of streamlined tubes intended for use in polymer heat exchangers is presented. The mechanical analysis considers the case in which the outer tube shape must remained streamlined (i.e. deformation is limited) and the inner flow passage is designed for optimal thermal performance. This combination of requirements is a particular challenge for polymer materials. The key to the mechanical analysis is use of dimensionless parameters including two dimensionless length scales, which characterize the tube geometry, and the ratio $\varepsilon_{\max} E/P_i$, which captures the effect of material stiffness and loading. Using this approach, a set of design curves can be generated from which combinations of tube geometry and materials can be selected that satisfy the deformation constraint. Once specific geometries that satisfy the mechanical constraint are identified, thermal performance such as the shape tube efficiency can be evaluated.

The method was demonstrated for elliptical tubes of non-uniform wall thickness. A finite element solution for the strain as a function of the tube material and geometry was determined for several geometries and a family of design curves for elliptical tubes was created.

References

1 Bigg, D. M., Stickford, G. H., and Talbert, S. G. Applications of polymeric materials for condensing heat exchangers. Polym. Engng Sci., 1989, 29(16), 1111–1116.

2 El-Dessouky, H. T. and Ettouney, H.M. Plastic/compact heat exchangers for single-effect desalination systems. Desalination, 1999, 122(2–3), 271–289.

3 Jachuck, R. J. J. and Ramshaw, C. Process intensification: polymer film compact heat exchanger (PFCHE). Chem. Engng Res. Des., 1994, 72(A2), 255–262.

4 Davidson, J. H., Oberreit, D., Liu, W., and Mantell, S. C. Are plastic heat exchangers feasible for solar water heaters? Part I: a review of the technology, codes and standards, and commercial products. ASME–KSME– JSME–ASHRAE–JSES International Renewable and Advanced Energy Systems for the 21st Century, CDROM, RAES99-7683, Maui, Hawaii, April 1999.

5 Li, Z., Davidson, J. H., and Mantell, S. M. Heat transfer enhancement using shaped polymer tubes: fin analysis. Trans. ASME, J. Heat Transfer, 2004, 126(2), 211–218.

6 Matos, R. S., Vargas, J. V. C., Laursen, T. A., and Saboya, F. E. M. Optimization study and heat transfer comparison of staggered circular and elliptic tubes in forced convection. Int. J. Heat Mass Transfer, 2001, 44(20), 53– 61.

7 Ota, T., Aiba, S., Tsuruta, T., and Kaga, M. Forced convection heat transfer from an elliptic cylinder ofaxis ratio 1: 2. Bull. Japan Soc. Mech. Engrs, 1983, 26(212), 262–267.

8 Ota, T. and Nishiyama, H. Heat transfer and flow around an elliptic cylinder. Int. J. Heat Mass Transfer, 1984, 27(10), 1771–1779.

9 Ruth, E. K. Experiments on a cross flow heat exchanger with tubes of lenticular shape. Trans. ASME, J. Heat Transfer, 1983, 105, 571–575.

10 Ru¨hlich, I. and Quack, H. New regenerator design for cryocoolers. In Proceedings of the 17th International Cryogenic Engineering Conference, Bournemouth,1998, pp. 291–294.

11 Ru¨hlich, I. and Quack, H. Investigations on regenerative heat exchangers. In Proceedings of the 10th International Cryocooler Conference, Monterey, California, 1999, pp. 265–274.

12 Zukauskas, A. and Ziugzda, J. Heat Transfer of a Cylinder in Cross flow, 1985, p. 150 (Hemisphere, New York).

13 Holland, M. Pressurized member with elliptic median line: effect of radial thickness function. J. Mech. Engng Sci., 1976, 18(5), 245–253.

14 Wu, C., Mantell, S. C., and Davidson, J. H. Polymers for solar domestic hot water: long-term performance of PB and Nylon6,6 tubing in hot water. J. Solar Energy Engng, 2004, 126, 581–586.

15 Timoshenko, S. Strength of Materials, 1955, p. 389 (Van Nostrand, Princeton, New Jersey).

16 Holland, M. Pressurized non-circular member: effect of mean-line form. J. Strain Analysis, 1982, 17(4), 237–241.

17 Romano, F. Non-circular rings under radial load. J. Franklin Inst., 1964, 277(5), 444–463.

18 Holland, M., Lalor, M. J., and Walsh, J. Principal displacements in a pressurized elliptic cylinder: theoretical predictions with experimental verification by laser interferometry. J. Strain Analysis, 1974, 9(3), 159–165.

19 ASTM Standard D 1598: Standard test method for time to failure of plastic pipe under constant internal pressure. In Annual Book of ASTM Standards, 1999 (American Society of Testing and Materials, Philadelphia, Pennsylvania).

20 Bhatti, M. S. Heat transfer in the fully developed region of elliptical ducts with uniform wall heat flux. Trans. ASME, J. Heat Transfer, 1984, 106, 895–898.

APPENDIX

Notation

A_i cross-sectional area of the inner flow passage (m^2)
D_h hydraulic diameter of an elliptical tube (m)
E Young's modulus (Pa)
h_o overall outer heat transfer coefficient (W/m^2 K)
k_w thermal conductivity (W/m K)
L_i length of the semi major axis of the inner surface of the tube (m)
L_o length of the semi major axis of the outer surface of the tube (m)
n vector normal to the wall
Nu Nusselt number
Pi internal fluid pressure (Pa)
P_{inner} inner perimeter (m)
Pr Prandtl number evaluated at the fluid bulk temperature
Pr_w Prandtl number evaluated at the tube wall surface temperature
q heat flux (W/m^2)
Q heat transfer rate per unit length tube (W)
r radial coordinate (m)
r_i length of the semi minor axis of the inner surface of the tube (m)
r_o length of the semi minor axis of the outer surface of the tube (m)
Re Reynolds number
t_{90} wall thickness at $\theta = 90^o$ (m)

T_{inner} fluid temperature inside the tube (K)
T_{outer} fluid temperature outside the tube (K)
U outer cross-flow air velocity (m/s)

ε von Mises strain
η shaped tube efficiency
θ angular coordinate of a point on the ellipse (deg)
λ_i length ratio of the minor axis to the major axis of the inner surface = r_i/L_i
λ_o length ratio of the minor axis to the major axis of the outer surface = r_o/L_o
λ_t length ratio of the wall thickness t_{90} to the outer semi minor axis = t_{90}/r_o
v Poisson's ratio
σ von Mises stress (Pa)

Subscripts

f fluid
max maximum value
w wall material
wall tube wall